Monthly Notices of the ROYAL ASTRONOMICAL SOCIETY LETTERS

Mon. Not. R. Astron. Soc. **405,** L41–L45 (2010) doi:10.1111/j.1745-3933.2010.00855.x

The nuclear stellar disc in Andromeda: a fossil from the era of black hole growth

Philip F. Hopkins★ and Eliot Quataert

Department of Astronomy and Theoretical Astrophysics Center, University of California Berkeley, Berkeley, CA 94720, USA

Accepted 2010 March 17. Received 2010 March 15; in original form 2010 February 4

ABSTRACT

The physics of angular momentum transport from galactic scales (∼10–100 pc) to much smaller radii is one of the outstanding problems in our understanding of the formation and evolution of supermassive black holes (BHs). Seemingly unrelated observations have discovered that there is a lopsided stellar disc of unknown origin orbiting the BH in M31, and possibly many other systems. We show that these nominally independent puzzles are in fact closely related. Multiscale simulations of gas inflow from galactic to BH scales show that when sufficient gas is driven towards a BH, gravitational instabilities form a lopsided, eccentric disc that propagates inwards from larger radii. The lopsided stellar disc exerts a strong torque on the remaining gas, driving inflows that fuel the growth of the BH and produce quasar-level luminosities. The same disc can produce significant obscuration along many sightlines and thus may be the putative 'torus' invoked to explain obscured active galactic nuclei and the cosmic X-ray background. The stellar relic of this disc is long lived and retains the eccentric pattern. Simulations that yield quasar-level accretion rates produce relic stellar discs with kinematics, eccentric patterns, precession rates and surface density profiles in reasonable agreement with observations of M31. The observed properties of nuclear stellar discs can thus be used to constrain the formation history of supermassive BHs.

Key words: galaxies: active – quasars: general – galaxies: evolution – cosmology: theory.

1 INTRODUCTION

A massive black hole (BH) resides at the centre of most massive galaxies (Kormendy & Richstone 1995; Gebhardt et al. 2000; Merritt & Ferrarese 2001). A long-standing problem in understanding their origin is how gas loses angular momentum and inflows from galactic scales to the BH. On large scales collisions with other galaxies and global instabilities can bring the gas down to radii (∼10–100 pc) where the gravitational force of the BH begins to dominate the dynamics (Shlosman, Frank & Begelman 1989; Barnes 1998; Schweizer 1998). However, the BH efficiently suppresses disturbances from larger scales. How, then, does the gas continue to flow in? On the smallest scales (≪0.1 pc), accretion can occur through angular momentum transport by local magnetic stresses (Balbus & Hawley 1998). But this leaves a critical gap of a factor of $\sim 10^2$–10^3 in radius, in which gas is still weakly self-gravitating and can form stars, but both larger scale torques and local magnetic stresses are inefficient; models have traditionally had great difficulty in crossing this gap (Shlosman & Begelman 1989; Goodman 2003; Thompson, Quataert & Murray 2005).

Independent observations of the properties of stars close to BHs in nearby galaxies have discovered that many of the old stars reside in an eccentric, lopsided stellar disc on spatial scales from ∼1 to 10 pc (Lauer et al. 1996, 2005; Thatte, Tecza & Genzel 2000; Debattista et al. 2006; Houghton et al. 2006). The most well-known and well-studied case is in the Andromeda galaxy, M31 (Lauer et al. 1993; Tremaine 1995; Bender et al. 2005). The dynamics of this disc have received considerable attention, but its origin remains poorly understood (Peiris & Tremaine 2003; Salow & Statler 2004; Bender et al. 2005). Given the demanding resolution requirements, it is also not clear whether such features are peculiar or generic.

To understand the angular momentum transport required for massive BH growth, we have recently carried out a series of numerical simulations of inflow from galactic to BH scales (Hopkins & Quataert 2009).[1] By resimulating the central regions of galaxies, gas flows can be followed from galactic scales of ∼100 kpc to ultimate spatial resolution <0.1 pc. For sufficiently gas-rich discy systems, gas inflow continues all the way to $\lesssim$0.1 pc. Near the radius of influence of the BH, the systems become unstable to the formation of lopsided, eccentric gas+stellar discs. This eccentric pattern is the

★E-mail: phopkins@astro.berkeley.edu

[1] Movies of these simulations are available at http://www.cfa.harvard.edu/phopkins/Site/Movies_zoom.html.

dominant mechanism of angular momentum transport at $\lesssim$10 pc, and can lead to accretion rates as high as $\sim 10\,M_\odot\,yr^{-1}$. Through this process, some of the gas continuously turns into stars and builds up a nuclear stellar disc. In this Letter, we examine the possibility that the nuclear stellar discs seen in M31 and other galaxies are 'fossils' from the era of BH growth. If correct, this provides a powerful new set of constraints on the formation and evolution of supermassive BHs.

2 THE SIMULATIONS

Hopkins & Quataert (2009) give a detailed description of the simulations used here. The simulations were performed with the parallel TreeSPH code GADGET-3 (Springel 2005). They include stellar discs and bulges, dark matter halos, gas and BHs. Here we wish to isolate the physics of gas inflow, so we do not include models for BH accretion and feedback – the BH's mass is constant in time and its only dynamical role is via its gravitational influence on scales $\lesssim$10 pc.

Because of the large dynamic range in both space and time needed for the self-consistent simulation of galactic inflows we use a 'zoom-in' resimulation approach. This begins with a suite of simulations of galaxy–galaxy mergers, and isolated bar-(un)stable discs. These simulations have 0.5×10^6 particles, corresponding to a spatial resolution of 50 pc. These simulations have been described in a series of previous papers (Cox et al. 2006; Robertson et al. 2006; Younger et al. 2008; Hopkins et al. 2009). From this suite, we select representative simulations of gas-rich major mergers of Milky Way mass galaxies (baryonic mass $10^{11}\,M_\odot$), and their isolated but bar-unstable analogues, to provide the basis for our resimulations. The dynamics on smaller scales does not depend critically on the details of the larger scale dynamics. Rather, the small-scale dynamics depends primarily on global parameters, such as the total gas-mass channelled to the centre relative to the pre-existing bulge mass.

Following gas down to the BH accretion disc requires much higher spatial resolution. We begin by selecting snapshots from the galaxy-scale simulations at key epochs. In each, we isolate the central 0.1–1 kpc region, which contains most of the gas that has been driven in from large scales. Typically this is about $10^{10}\,M_\odot$ of gas, concentrated in a roughly exponential profile with a scalelength of $\sim$0.3–0.5 kpc. From this mass distribution, we then repopulate the gas in the central regions at much higher resolution, and simulate the dynamics for several local dynamical times. These simulations involve 10^6 particles, with a resolution of a few pc and particle masses of $\approx 10^4\,M_\odot$. We have run $\sim$50 such resimulations, corresponding to variations in the global system properties, the model of star formation and feedback and the exact time in the larger scale dynamics at which the resimulation occurs. Hopkins & Quataert (2009) present a number of tests of this resimulation approach and show that it is reasonably robust for this problem. This is largely because, for gas-rich discy systems, the central $\sim$300 pc becomes strongly self-gravitating, generating instabilities that dominate the subsequent dynamics.

These initial resimulations capture the dynamics down to $\sim$10 pc, still insufficient to quantitatively describe accretion on to a central BH. We thus repeat our resimulation process once more, using the central $\sim$10–30 pc of the first resimulations to initialize a new set of even smaller scale simulations. These typically have $\sim 10^6$ particles, a spatial resolution of 0.1 pc, and a particle mass $\approx 100\,M_\odot$. We carried out $\sim$50 such simulations to test the robustness of our conclusions and survey the parameter space of galaxy properties. These final resimulations are evolved for $\sim 10^7$ yr – many dynamical times at 0.1 pc, but very short relative to the dynamical times of the larger scale parent simulations.[2]

Our simulations include gas cooling and star formation, with gas forming stars at a rate motivated by the observed Kennicutt (1998) relation. We use a star formation rate per unit volume $\dot{\rho}_* \propto \rho^{3/2}$, with normalization chosen so that a Milky Way like galaxy has a total star formation rate of about $1\,M_\odot\,yr^{-1}$. Because we cannot resolve the detailed processes of supernovae explosions, stellar winds and radiative feedback, feedback from stars is modelled with an effective equation of state (Springel & Hernquist 2003). In this model, feedback is assumed to generate a non-thermal (turbulent) sound speed; we use subgrid sound speeds $\sim$20–100 km s^{-1}, motivated by a variety of observations of dense, star forming regions (Downes & Solomon 1998; Bryant & Scoville 1999; Förster Schreiber et al. 2006; Iono et al. 2007). Within this range, we found little difference in the physics of angular momentum transport or in the resulting accretion rates, gas masses, etc. (see also Section 3 Hopkins & Quataert 2009).

3 RESULTS

Fig. 1 shows an example of the results of our resimulations. We follow the merger and coalescence of two Milky Way mass galaxies, an event chosen because it is likely to lead to rapid BH growth. The first image (top left) provides a large-scale view of the system just after the coalescence of the two galactic nuclei. The highly asymmetric disturbances efficiently torque the gas. Inside the central $\sim$kpc, the inflowing gas piles up at the point where its gravity begins to dominate that of the stars and dark matter; this dense gas generates a burst of star formation. Precisely because the gas and newly formed stars are self-gravitating, they form secondary gravitational instabilities such as bars and spiral waves that produce further torques and inflow. This is essentially the 'bars within bars' mechanism proposed in Shlosman et al. (1989) and it occurs for the reasons outlined therein. But once the gas reaches $\sim$10 pc, this mechanism no longer works – the gravity of the BH begins to dominate ($M_{\rm BH} = 3 \times 10^7\,M_\odot$ here) and the system can no longer support the large-scale bars critical to the inflow on larger scales.

At precisely these scales our simulations demonstrate that a new instability generically arises – a nearly static (slowly precessing) lopsided or eccentric disc of gas and stars. Such slowly varying eccentric ($m = 1$) perturbations are unique to the gravitational field of a point mass such as a BH. But they are also linearly stable (Tremaine 2001), so how do they arise in the simulations? We discuss this in detail in Hopkins & Quataert (2009); the mode is a *global* phenomena that grows from the outside in. It first starts to grow because of self-gravity, where the mass of the (stellar+gas) disc is comparable to the mass of the BH (at $\sim$10–100 pc). Gas moving in circular orbits passes through this eccentric disc, and experiences a torque from the stars therein, causing the gas to lose angular momentum and fall inwards. Some of the gas turns into stars, those stars are excited into the $m = 1$ mode, allowing the perturbation to efficiently propagate inwards to $\sim$0.1 pc. Although at radii where $M_{\rm disc}(<R) \ll M_{\rm BH}$, the system may formally be stable, the eccentric pattern is *induced* by the mass distribution at somewhat larger radii. The lopsided or eccentric disc, then, is a coherent

[2] We also carried out a few extremely high-resolution intermediate-scale simulations, which include $\sim 5 \times 10^7$ particles and resolve structure from $\sim$kpc to $\sim$0.3 pc – these obviate the need for a second zoom-in iteration and yield identical conclusions.

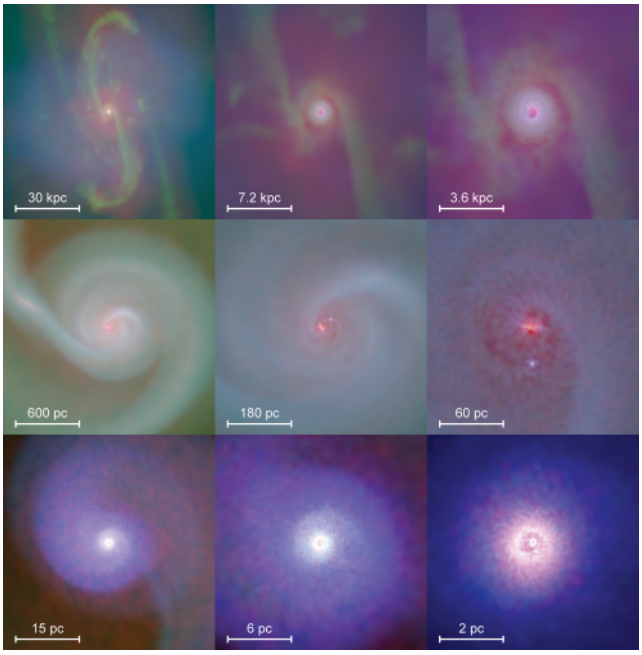

Figure 1. Example simulation: red colours denote stellar mass density, green-to-blue the gas density with increasing specific star formation rate. Each projects the rotating gas face-on. Top: galaxy-scale: galaxy–galaxy merger just after nuclear coalescence [$10^{11}\,M_\odot$, gas fraction $f_{\rm gas} \sim 0.4$, initial $B/T = 0.2$; simulation b3ex(co) in Hopkins & Quataert 2009]. The merger has driven large amounts of gas to $\sim$1 kpc, forming a nuclear starburst. Middle: re-simulation of the $\sim$0.1–1 kpc region (simulation If9b5). The (self-gravitating) starburst disc develops a spiral/bar mode that drives gas to $\sim$10 pc, where the bar is suppressed by the gravity of the BH. Bottom: re-simulation of the central $\sim$30 pc (simulation Nf8h1c1qs). The inflow to these scales forms a lopsided eccentric disc around the BH (mapping to a one-armed spiral at larger radii). The disc drives accretion rates of $\sim$1–10 $M_\odot\,{\rm yr}^{-1}$ to < 0.1 pc, and leaves the stellar relics shown in Figs 2 and 3.

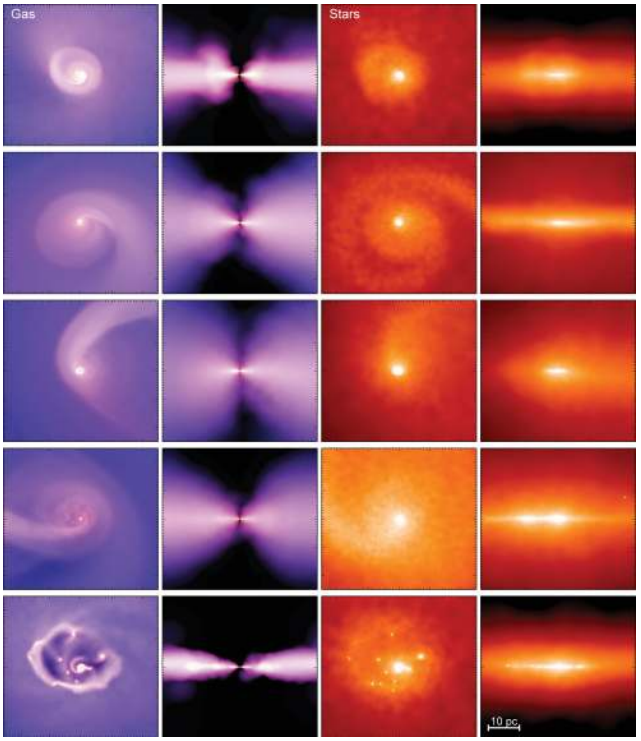

Figure 2. Nuclear disc in typical simulations. Scale is the same (lower right). Rows show simulations of the central $\sim$50 pc of galactic nuclei with different galaxy properties [top to bottom: Nf8h1c0thin, Nf8h1c1thin, Nf8h1c1qs, Nf8h1c1dens, Nf8h1c0 in Hopkins & Quataert (2009), which have initial $f_{\rm gas} \sim 0.5$–0.8, $h/R = 0.16, 0.08, 0.28, 0.25, 0.15$, $M_{\rm BH} \sim 3 \times 10^7\,M_\odot$, and initial discy mass $\sim$1.2, 1.7, 3.0, 8.1, $0.25 \times 10^7\,M_\odot$ inside 10 pc], and different treatments of stellar feedback (sub-grid sound speeds $c_{\rm s} \sim 35$, 20, 40, 50, 10 km s^{-1} from top to bottom). The formation of a lopsided disc is ubiquitous. Left: gas surface density. Colours encode absolute star formation rate (increasing blue to yellow). Gas shocks (sharp edges) dissipate energy, leading to rapid inflow. Middle left: same, edge-on in cylindrical $(R,\ z)$ coordinates to emphasize the disc thickness versus radius. Gravitationally driven turbulence results in the discs always being somewhat thick on these scales, even with negligible stellar feedback (bottom row). Middle right: as *left*, but showing the stellar mass distribution. Lack of shocks means the edges of the disc are less sharp, but they are still clear. Right: edge-on stellar density $(x,\ z)$. Several of the systems appear to have two nuclei: the initial indication of the eccentric disc in M31 (P1/P2 feature).

global pattern superimposed on the otherwise axisymmetric gas and stellar mass distribution. The eccentric pattern precesses with an angular pattern speed $\Omega_{\rm p}$, which we measure to be $\sim$1–5 km s^{-1} pc^{-1} (independent of radius), set by the rotation rate at the radii where the disc and BH masses are comparable.

We have run a suite of over $\sim$50 simulations in order to study the properties of, and robustness of, the eccentric discs in our calculations. Fig. 2 shows face-on and edge-on views of the gas and stars in several of these simulations. Provided that a significant amount of gas ($\gtrsim$10% $M_{\rm BH}$) can be driven in from larger radii by global torques in galaxies, eccentric nuclear discs are generic.

As the flow of gas subsides, a stellar remnant will remain that can retain the eccentric pattern. The characteristic radii $\sim$1–10 pc and stellar masses $\sim$0.1–1 $M_{\rm BH}$ of the eccentric nuclear discs in our simulations are consistent with those observed in M31 and other systems. Fig. 2 shows stellar density maps for several of our simulations, including those that have exhausted most of their gas. The distinct nuclear disc is evident. In an edge-on projection, several of these nuclear discs appear to have double nuclei (secondary brightness peaks) – this is caused by the high density of stars near apocentre in their elliptical orbits. In several cases, this closely resembles the secondary brightness peak in M31 (the P1 feature), believed to arise in the same manner; note in particular the second-from-bottom edge-on panel, where the two peaks are close in brightness and separated by $\sim$4 pc. We confirm the inference from models of P1 that the appearance of secondary nuclei is sensitive to projection effects, and usually requires a sightline reasonably close to edge-on.

Fig. 3 shows the velocity field of the stars in these relics, long after the gas is exhausted, and scaled as if observed at the centre of M31; the data for M31 are in the bottom panel. The overall agreement is impressive, particularly given that these simulations are not designed to reproduce the observed features of M31 in any way, but rather to study the growth of massive BHs. We find similar agreement when comparing to observations of the nuclear disc in NGC 4486b (Lauer et al. 1996). The rotational velocity field of M31 is slightly less symmetric than our 'average' simulation, but a number agree quite closely, and the level of dispersion asymmetry observed is typical for our simulations.

Fig. 4 compares a number of the properties of our simulated relic stellar discs with those of the M31 system (Jacobs & Sellwood 2001; Salow & Statler 2001; Sambhus & Sridhar 2002; Peiris & Tremaine 2003; Salow & Statler 2004). The range of simulations includes variations in initial conditions and the treatment of stellar

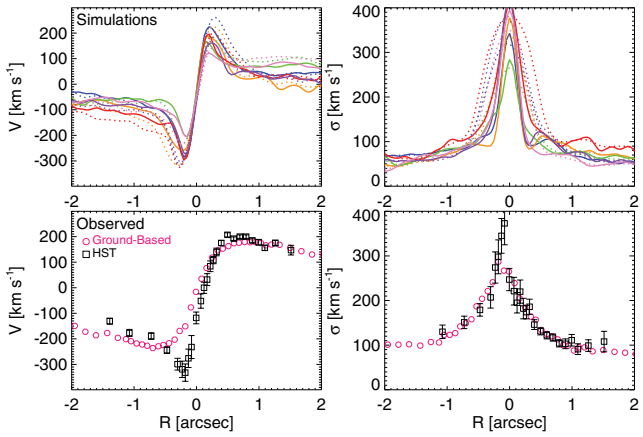

Figure 3. Top: mean projected line-of-sight velocity V (left) and velocity dispersion σ (right) of the relic nuclear stellar discs in our simulations, long after gas is exhausted. Each solid line is a mock line-of-sight velocity field of the stars, as if they were at the distance and viewing angle of the M31 nucleus (54° from edge-on; Peiris & Tremaine 2003). Dotted lines vary the inclination angle by 10°. Velocities are measured in narrow radial pixels along a major-axis slit matched in pixel size, width and resolution to the observations. Bottom: observations of M31. Our mock profiles are matched to the resolution of the *Hubble Space Telescope* observations shown here (black squares) (Bender et al. 2005). Magenta circles are ground-based observations (Kormendy & Bender 1999) which extend to larger radii but have inferior resolution and smooth the velocity field at $|R| < 1$ arcsec.

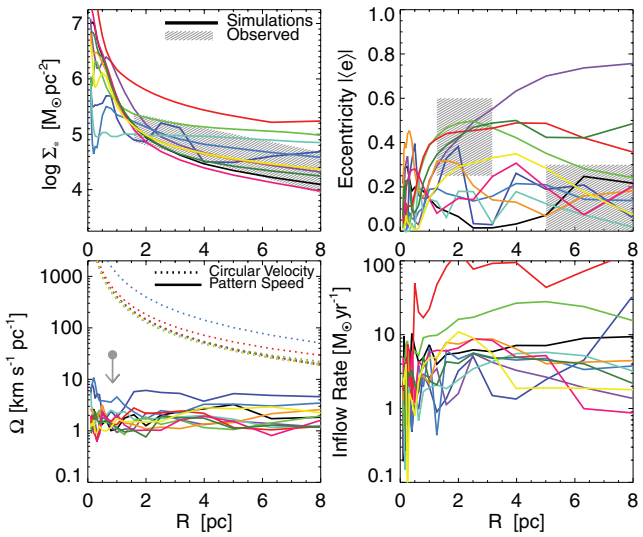

Figure 4. Properties of the simulated nuclear stellar discs versus radii, over the observed scales in M31. Each solid line corresponds to a simulation, as in Fig. 3. Where available, we compare with the properties of the M31 system inferred from observations (grey shaded regions). Top left: stellar mass surface density. Top right: mean eccentricity of the disc along its major axis. Bottom left: angular pattern speed (precession rate) of the disc, which is much less than the angular velocity of individual stars in the disc (dotted lines). Bottom right: inflow rate of gas driven by the gravitational torques of the eccentric disc itself, during the active phase when the disc formed. This accretion can produce most of the BH growth.

feedback. The plotted surface densities are azimuthally averaged (this suppresses the double-peaked appearance of the simulations and M31, but is more robust to projection effects). Note that the pattern speed Ω_p in our simulations is quite low $\approx$1–5 km s^{-1} pc^{-1} (lower left), much less than the rotation rate of individual stars at small radii. The pattern speed is set at the large radii where the eccentric mode begins. The actual precession rate in M31 is not very well constrained, but most studies place an upper limit of $<$30 km s^{-1} (Sambhus & Sridhar 2000), and several studies imply a value close to our prediction (see Bacon et al. 2001). The mean disc eccentricity in the simulations is also in broad agreement with that observed, although this varies significantly from one simulation to another.

Fig. 4 also shows the inflow rates generated by the nuclear stellar disc during its gas-rich phase. Nuclear discs similar to M31 generate accretion rates up to several M$_\odot$ yr^{-1} during the quasar epoch, when they are gas rich. This highlights the key role that eccentric stellar discs can play in fuelling BH growth.

Our models include a very simplified sub-grid treatment of the feedback from supernovae and massive stars. To test the impact of this on our results, we carried out calculations with identical initial conditions and turbulent velocities ranging from $\sim$10 to 100 km s^{-1}, roughly the lower and upper limits allowed by observational constraints for the systems of interest (see fig. 1 of Hopkins & Quataert 2009 and references therein). The value of the subgrid sound speed has a significant effect on the amount of resolved substructure in the simulation, with more substructures present in simulations with lower turbulent velocities. This is not surprising since larger turbulent velocities raise the Jeans mass/length, above which gravity is the dominant force. However, all of the simulations show a similar nuclear lopsided disc. In terms of the properties shown in Figs 3 and 4, the differences produced by changing the subgrid model are similar to the differences produced by somewhat different galaxy properties. The reason for the weak dependence on the subgrid model is that the torques in our simulations are primarily determined by gravity, not hydrodynamic forces or viscosity (see Hopkins & Quataert 2009). The primary role of the feedback model is simply to prevent catastrophic fragmentation of the galactic gas.

4 DISCUSSION

Hopkins & Quataert (2009) argue that the dominant mechanism of angular momentum transport in gas-rich galactic nuclei, from near the BH radius influence ($\sim$10 pc) down to the Keplerian viscous accretion disc ($\ll$0.1 pc), is gravitational torques produced by an eccentric, lopsided disc (an $m = 1$ mode); this asymmetric disc forms in our simulations when the disc mass is at least $\sim$10 per cent of the BH mass. These torques provide the 'missing link' connecting the gas reservoir on galactic scales to the small-scale accretion disc. In this Letter, we have shown that the long-lived ('fossil') stellar relics of these discs are remarkably similar to the eccentric stellar disc observed around the BH in M31. This suggests that the stellar kinematics and morphology in galactic nuclei can provide new insights into the physics of BH growth.

Emboldened by our success, we can use the observed properties of the M31 disc to infer the accretion it was responsible for. If the M31 disc was at one point gas rich, the eccentric pattern in the stars would produce strong torques in the gas, leading to an accretion rate of $\dot{M} \sim \Sigma_{\rm gas}\, R^2\, \Omega\, |\Phi_1/\Phi_0|$, where Φ_1 and Φ_0 are the asymmetric and axisymmetric terms in the gravitational potential, respectively. For the measured BH mass (10^8 M$_\odot$; Bender et al. 2005) and potential of the eccentric disc (Peiris & Tremaine 2003), this implies an accretion rate of $\sim$1 M$_\odot$ yr^{-1}, close to the Eddington limit of 2.4 M$_\odot$ yr^{-1}. More directly, we find that simulations that yield stellar relics in closest agreement with M31 have typical inflow rates at $R \lesssim 0.1$ pc in their active phases of $\sim$0.3–5 M$_\odot$ yr^{-1} (Fig. 4).

These accretion rates imply that the observed stellar disc could have helped the M31 BH gain much of its mass.

During the gas-rich phase, the typical column density of gas for an edge-on line of sight through the disc is $N_{\rm H} \sim 10^{25-26}$ atoms cm^{-2}, sufficient to obscure radiation from the BH even in the X-rays. A combination of gravitational perturbations and stellar feedback generate large 'random' motions in the gas: the discs are thus thick, with column densities sufficient to block the optical light ($N_{\rm H} \gtrsim 10^{22}$ atoms cm^{-2}) out to an angle $\sim$20°–45° above the plane – in other words, a fraction $\sim$30–60 per cent of all sightlines will be obscured by gas and dust in the nuclear disc. The properties of the obscuring disc we infer are strikingly similar to those invoked for the canonical 'toroidal obscuring region,' assumed to account for most of the obscured active galactic nucleus (AGN) population (Lawrence 1991; Antonucci 1993; Urry & Padovani 1995). In the context of our model, the observed ubiquity of the torus suddenly has a dynamical origin: it itself helps drive the accretion.

Understanding the longevity of the eccentric disc in M31 has been as challenging as understanding its origin. Differential precession should lead to phase mixing that ultimately wipes out the coherent eccentricity of the disc. Indeed, we do see that the eccentric pattern damps away at larger radii; however, the pattern at radii $\sim$ pc, where the M31 disc is observed, persists in our simulations as long as they can be reliably evolved, for 10^8 yr, which is $\sim 10^4$ dynamical times. Self-gravity is likely to help maintain the pattern even longer, in principle for much longer than the age of the universe (Bacon et al. 2001; Jacobs & Sellwood 2001; Salow & Statler 2004).

Our simulations demonstrate that eccentric stellar and gaseous discs form whenever the mass in the discy component in the central $\sim$10–30 pc is comparable to that of the BH (Hopkins & Quataert 2009). It is unclear, however, under what conditions these nuclear stellar discs will survive to the present day. Their long-term stability in isolation is not fully understood. In addition, it is easy to imagine that subsequent 'dry' galaxy mergers might destroy these features. This is a key question for future research. Observationally, there are a number of candidate systems in addition to M31, as evidenced by apparently offset centres, 'hollow' central light profiles, double nuclei, or chemically distinct secondary nuclei (Thatte et al. 2000; Afanasiev & Sil'chenko 2002; Lauer et al. 2002, 2005; Debattista et al. 2006), and NGC 4486b is another confirmed eccentric disc (Lauer et al. 1996). There may be similar features in nuclear gas discs as well (Seth et al. 2010). But eccentric discs clearly do not exist in all systems, as evidenced by the nucleus of M32. More detailed observational constraints on the fraction of galaxies with old, asymmetric nuclear stellar discs would provide a strong constraint on our models.

When nuclear eccentric discs do survive, our models imply that there should be a correspondence between the properties of the nuclear stellar disc and the central BH mass, as we have demonstrated is the case in M31. Very low pattern speeds <10 km s^{-1} pc^{-1} should be ubiquitous, as they are required for efficient exchange of angular momentum between the stars and gas. If some gas flows in from larger radii, or accumulates via stellar evolution, the nuclear regions can experience recurrent low-level AGN activity and/or star formation, regulated by the same mechanism of eccentric stellar torques (e.g. M31's young stellar population, Chang et al. 2007). Such episodes may complicate dating the formation epochs of these discs, but also provide a laboratory to study the physics of inflow in detail. The properties of the nuclear disc in its gas-rich phase determine the distribution of implied torus scalelengths and gas densities, which can be probed by infrared adaptive optics observations of nearby bright AGN (Davies et al. 2007; Hicks et al. 2009). On the theoretical side, improvements in the treatment of gas physics and star formation will enable more detailed comparison with observations.

ACKNOWLEDGMENTS

We thank Phil Chang, Lars Hernquist, Scott Tremaine, John Kormendy and Tod Lauer for helpful discussions during the development of this work. Support for PFH and EQ was provided by the Miller Institute for Basic Research in Science, University of California Berkeley. EQ was also supported in part by NASA grant NNG06GI68G and the David and Lucile Packard Foundation.

REFERENCES

Afanasiev V. L., Sil'chenko O. K., 2002, A&A, 388, 461
Antonucci R., 1993, ARA&A, 31, 473
Bacon R. et al., 2001, A&A, 371, 409
Balbus S. A., Hawley J. F., 1998, Rev. Modern Phys., 70, 1
Barnes J. E., 1998, Saas-Fee Advanced Course 26. Springer, p. 275
Bender R. et al., 2005, ApJ, 631, 280
Bryant P. M., Scoville N. Z., 1999, AJ, 117, 2632
Chang P. et al., 2007, ApJ, 668, 236
Cox T. J. et al., 2006, ApJ, 650, 791
Davies R. I. et al., 2007, ApJ, 671, 1388
Debattista V. P. et al., 2006, ApJ, 651, L97
Di Matteo T., Springel V., Hernquist L., 2005, Nat, 433, 604
Downes D., Solomon P. M., 1998, ApJ, 507, 615
Förster Schreiber N. M. et al., 2006, ApJ, 645, 1062
Gebhardt K. et al., 2000, ApJ, 539, L13
Goodman J., 2003, MNRAS, 339, 937
Hicks E. K. S. et al., 2009, ApJ, 696, 448
Hopkins P. F. et al., 2009, ApJ, 691, 1168
Hopkins P. F., Quataert E., 2009, MNRAS, in press (arXiv:0912.3257)
Houghton R. C. W. et al., 2006, MNRAS, 367, 2
Iono D. et al., 2007, ApJ, 659, 283
Jacobs V., Sellwood J. A., 2001, ApJ, 555, L25
Kennicutt R. C. Jr, 1998, ApJ, 498, 541
Kormendy J., Bender R., 1999, ApJ, 522, 772
Kormendy J., Richstone D., 1995, ARA&A, 33, 581
Lauer T. R. et al., 1993, AJ, 106, 1436
Lauer T. R. et al., 1996, ApJ, 471, L79
Lauer T. R. et al., 2002, AJ, 124, 1975
Lauer T. R. et al., 2005, AJ, 129, 2138
Lawrence A., 1991, MNRAS, 252, 586
Merritt D., Ferrarese L., 2001, ApJ, 547, 140
Peiris H. V., Tremaine S., 2003, ApJ, 599, 237
Robertson B. et al., 2006, ApJ, 641, 90
Salow R. M., Statler T. S., 2001, ApJ, 551, L49
Salow R. M., Statler T. S., 2004, ApJ, 611, 245
Sambhus N., Sridhar S., 2000, ApJ, 539, L17
Sambhus N., Sridhar S., 2002, A&A, 388, 766
Schweizer F., 1998, Saas-Fee Advanced Course 26. Springer, p. 105
Seth A. C. et al., 2010, ApJ, in press (arXiv:1003.0680)
Shlosman I., Begelman M. C., 1989, ApJ, 341, 685
Shlosman I., Frank J., Begelman M. C., 1989, Nat, 338, 45
Soltan A., 1982, MNRAS, 200, 115
Springel V., 2005, MNRAS, 364, 1105
Springel V., Hernquist L., 2003, MNRAS, 339, 289
Thatte N., Tecza M., Genzel R., 2000, A&A, 364, L47
Thompson T. A., Quataert E., Murray N., 2005, ApJ, 630, 167
Tremaine S., 1995, AJ, 110, 628
Tremaine S., 2001, AJ, 121, 1776
Urry C. M., Padovani P., 1995, PASP, 107, 803
Younger J. D. et al., 2008, ApJ, 686, 815
Yu Q., Tremaine S., 2002, MNRAS, 335, 965

This paper has been typeset from a TEX/LATEX file prepared by the author.